frontiers in Energy Research

ORIGINAL RESEARCH
published: 09 December 2020
doi: 10.3389/fenrg.2020.537973

Investment Planning Methodology for Complex Urban Energy Systems Applied to a Hospital Site

Bastien Bornand[1]*, *Luc Girardin*[1], *Francesca Belfiore*[1], *Jean-Loup Robineau*[1], *Stéphane Bottallo*[2] and *François Maréchal*[1]

[1]Industrial Process and Energy Systems Engineering (IPESE-EPFL), École Polytechnique Fédérale de Lausanne, Lausanne, Switzerland, [2]Operations Department–Energy Sector, Geneva University Hospitals (HUG), Geneva, Switzerland

Industrial process integration based on mixed integer linear programming has been used for decades to design and improve industrial processes. The technique has later been extended to solve multi-period and multi-scale problems for the design of urban energy systems. Assistance is indeed required for the elaboration of coordinated investment scheduling strategies to promote renewable and efficient urban energy infrastructure shaping the future energy context for the next decades. Major energy consumers, such as hospital complexes, airports, or educational campuses can act as a driving force for the development of renewable energy cities by attracting profitable large-scale energy networks and infrastructure. The proposed methodology generates optimal alternatives for the replacement, in a long-term perspective, of the various energy supply units and systems considering the evolution of the energy demand and the availability of the energy resources. Energy integration techniques are coupled to a parametric multi-objective optimization routine to select and size the energy equipment with both financial profitability and CO_2 emission reduction as objectives. The originality of the developed method lies in the integration of a multi-period mixed integer linear programming formulation to generate long-term investment planning scenarios. The method has been demonstrated on a complex of eight hospitals totaling 466,000 m^2 and an operating budget of 1.85 billion USD per year. The energy integration of new centralized and decentralized equipment has been evaluated on a monthly basis over four periods until the year 2035. The results show that among the four scenarios identified, the most optimistic alternative allows to decrease the final energy consumption of about 36%, cut the CO_2 emissions by a half, multiply the renewable energy share by a factor 3.5 while reducing the annual total cost by 24%. This scenario considers mainly the integration of a very low temperature district heating with decentralized heat pumps to satisfy the heat requirements below 75°C, as well as heat recovery systems and the refurbishment of about 33% of the building stock.

Keywords: complex urban energy system, integrated energy systems, hospital, investment planning model, multi-objective multi-period optimization, process integration, 100% renewable energy systems, district heating and cooling

OPEN ACCESS

Edited by:
Jin Xuan,
Loughborough University,
United Kingdom

Reviewed by:
Andreas Koch,
European Institute for Energy Research, Germany
Hao Zhang,
The Univeristy of Edinburgh,
United Kingdom

***Correspondence:**
Bastien Bornand
bastienbornand@vonet.ch

Specialty section:
This article was submitted to Sustainable Energy Systems and Policies, a section of the journal Frontiers in Energy Research

Received: *26 February 2020*
Accepted: *22 September 2020*
Published: *09 December 2020*

Citation:
Bornand B, Girardin L, Belfiore F, Robineau J-L, Bottallo S and Maréchal F (2020) Investment Planning Methodology for Complex Urban Energy Systems Applied to a Hospital Site. Front. Energy Res. 8:537973. doi: 10.3389/fenrg.2020.537973

1. INTRODUCTION

Buildings are the largest end-use sector accounting for around 40% of the total final energy consumption in Europe (Gynther et al., 2015) and 36% in the world (IEA, 2018). According to the International Renewable Energy Agency, the share of clean district energy systems for building heat demand is projected to more than double by 2050 with a significant increase by 70% of the electricity demand in the sector (IRENA, 2018). The decarbonization of the energy resources employed would indeed require a large-scale electrification of the thermal utilities, combined with investments in efficient renewable technologies. Furthermore, increasing the 1–2% buildings' turnover (IEA, 2018) would unlock the powerful potential of buildings' retrofit to reduce energy consumption and pollutant emissions (Ascone et al., 2016). However, despite the recognized potential of the building sector within the energy system, there has been slow progress in renewable energy uptake in heating and cooling (Murdock et al., 2019).

To achieve effective energy transition toward renewable energy systems, the decision-making process needs to be tied to a long-term planning cycle integrating the life cycle of buildings and building systems (ASTM International, 2017). The crucial point here is that the selection of investment scheduling strategies shaping the energy future of the community for at least the next 25–50 years (ASHRAE, 2003). However, as the use of energy-efficient equipment and renewable energy technologies requires a higher initial investment than ordinary equipment and longer payback time (Wang et al., 2016), the commitment to long-term investment is disfavored by the current context of low-energy prices. This is especially true for those sectors in which the energy expenses represent only a minor share of the overall operating cost (e.g., in the hospital sector, they constitute less than 1%). In the perspective of refurbishment of the building stock and integration of new renewable energy sources, there is therefore a need for stepwise approaches and tools that allow to

- convince decision-makers to invest in the energy transition through coordinated selection and replacement of energy systems and equipment and
- conciliate operational constraints and energy performance actions through planning and coordination between the property master plan[a] and the state energy targets.

A starting point to establish renewable energy strategies is the development of synergies between major consumers and the surrounding districts. As full economical actors, major consumers are indeed acting as potential profitable magnets of urban-scale projects, since they could also be seen as "major energy suppliers."

Healthcare facilities are considered major energy consumers due to their combined need of reliable electricity and thermal energy to satisfy heating, cooling, air conditioning, lighting, and the use of medical and nonmedical equipment (Franco et al., 2017). Moreover, with respect to conventional buildings, these entities are subject to higher hygienic standards and stricter control of air temperature. Indeed, zones such as operating rooms require low temperature to ensure the comfort of personnel, specifically the surgeon (Hakim et al., 2018), while a higher air temperature [i.e., between 20 and 24°C according to international standards (Teke and Timur, 2014)] is required to assure the comfort of patients due to the lower metabolic rates caused by their physical inactivity (Franco et al., 2017).

Hospital districts represent a heterogeneous and complete case study in the aim of developing integrated energy planning methods. Researchers show that hospitals constitute the highest energy consumption per unit of floor area in the building sector (Buonomano et al., 2014; Ascone et al., 2016), with a share of approximately 6% of total energy consumption in the utility buildings sector (Franco et al., 2017). The large landscape of activities, combined with high hygienic standards and energy supply reliability prescriptions, are heavy constraints in the scope of large-scale and long-term energy optimization (Ascone et al., 2016). Moreover, the intrinsic nature of hospital activities, ubiquitous and unstoppable, further complicates the problems, making the research of the optimal operational scheduling a challenging task. On the other hand, there is a lack of data regarding measured and estimated energy consumption in hospital buildings (Buonomano et al., 2014), and databases must be enhanced.

The current work contributes to the long-term needs characterization, heat recovery potential, and resource availability assessment of major energy consumers, with the final goal of improving their integration within the urban sector, optimizing the mesh of energy flows at the district scale and properly scheduling the investments. The proposed method has been applied to the University Hospital of Geneva (HUG), which is a primary actor for the energy strategy of the surrounding district, as it is subject to important architectural morphing plan within the future 20 years (**Figures 1** and **2**).

This case study fits the legal definition of major energy consumer[b,] given by the state's law on energy (Republic and Canton of Geneva, 2010; Republic and Canton of Geneva, 2012), which also prescribes energy consumption standards and energy performance actions to be conducted adopting an exergy-based approach (Favrat et al., 2008).

2. STATE OF THE ART

2.1. Energy Integration for Urban Energy Planning

Energy integration approaches based on pinch analysis and mathematical programming have been extensively developed in the last decades (Liew et al., 2016; Liew et al., 2017). Mixed-integer linear programming (MILP) formulations using time slices have become a common method for the design and

[a] The property master plan includes all the renovation projects of the building stock defined by the property for the next 20 years as depicted in **Figure 2**.

[b] Consumer with an annual heat and electricity consumption greater than 5 GWh/yr or/and electricity consumption greater than 0.5 GWh/yr.

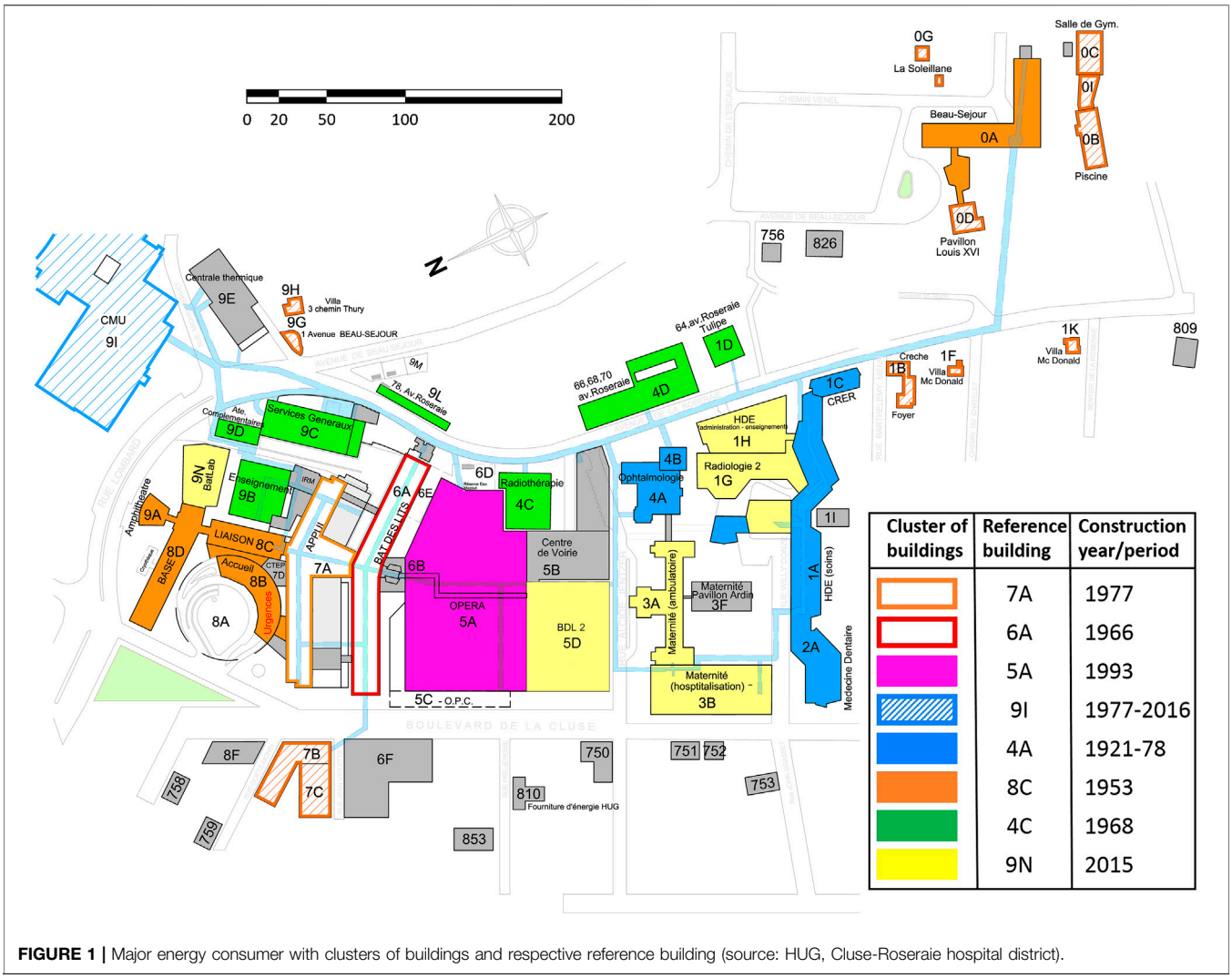

FIGURE 1 | Major energy consumer with clusters of buildings and respective reference building (source: HUG, Cluse-Roseraie hospital district).

optimization of urban multi-energy systems integrating variable energy supply and demand, district heating and cooling (DHC) networks, centralized/decentralized heat and power plants (Weber, 2008), and thermal storage (Rager, 2015). The computational complexity of solving multi-period heat cascades on a yearly basis in heterogeneous urban zones, mixing existing, new, and refurbished buildings, has been addressed using spatial and temporal data reduction techniques (Fazlollahi, 2014). Energy integration methods and tools, such as OsmoseLua (Yoo et al., 2015), have proven to be flexible enough to integrate complex energy conversion systems in cities (Suciu et al., 2018b). Attempt to use these techniques for long-term coordinated regional energy planning from the heat perspective up to horizon 2,100 has shown that long-term trends, such as cost and emission, can be accurately estimated using monthly time steps (Girardin et al., 2015).

However, meeting sustainability target in cities through energy planning is a complex task (Cajot et al., 2017) which not only relies on the use of sophisticated tools but also requires the analysis of combination of solutions in a framework that allows to better identify perspectives and integrate conflicting objectives while considering multiple geographical and temporal scales (Cajot and Schüler, 2019).

This study looks further ahead in the practical application by integrating, in a long-term perspective, intermittent renewable resources to satisfy both heating and cooling requirements. Moreover, clustering techniques and graphical representation are exploited to identify a limited number of long-term investment scenarios from a large set of generated alternative solutions.

2.2. Energy Integration in Hospital(s)

To the best of the authors' knowledge, despite the proven potential of energy integration techniques, their systematic application in the hospital site is still at an early stage of development. Integration methods have nevertheless been implemented on few real case studies, highlighting the relevance of pinch analysis (Herrera et al., 2003) and mathematical optimization. Biglia et al. (2017) developed a mathematical model through the energy hub methodology for the energy and economic analysis of large hospital complex,

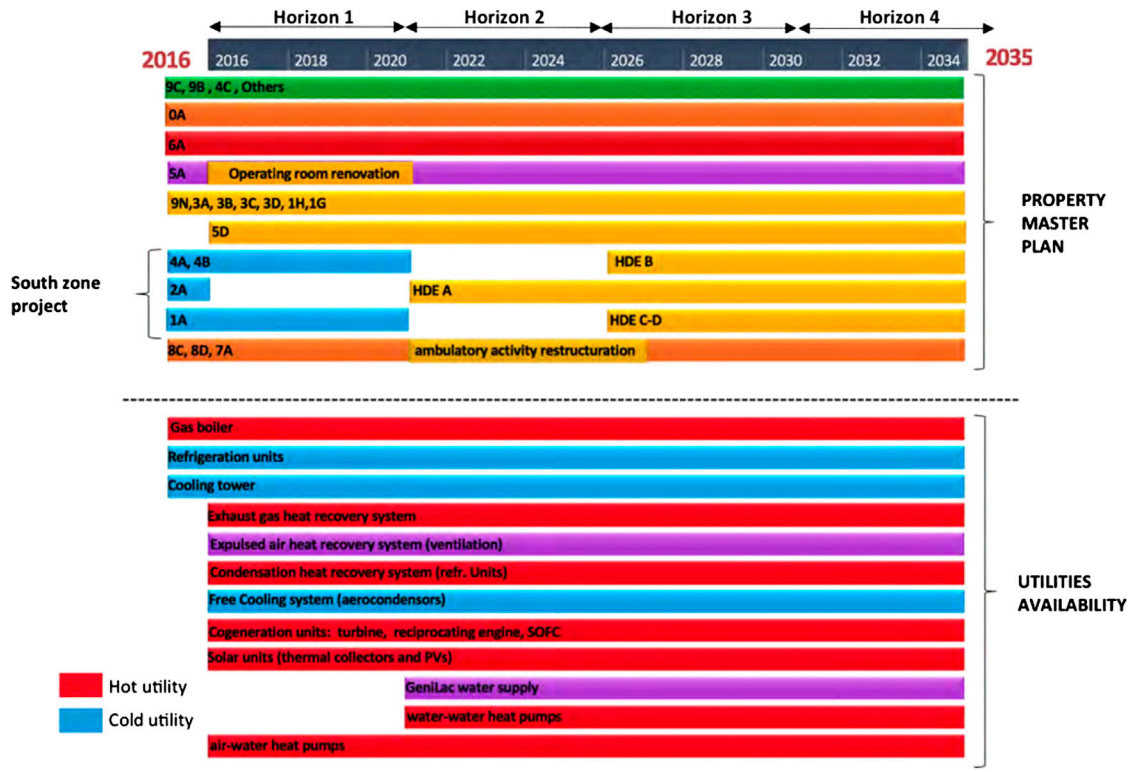

FIGURE 2 | Time horizons of the energy planning of Cluse-Roseraie hospital district, including the architectural projects planned by the property master plan (main activity morphing and refurbishment actions in yellow), the existing energy supply units, the new available technologies, and the urban-scale DHC project "GéniLac" in 2021. Colors refer to **Figure 1**.

applied to the hospital of Cagliari in Sardinia. The proposed method is based on monthly energy monitoring showing that including seasonal variation helps the process of equipment design and sizing. However, this approach considers non-evolving systems and does not include long-term planning aspects.

Several authors have investigated the integration of co- and trigeneration (CHCP) in healthcare facilities using MILP formulation to solve cost and pollutant emission optimization problems (Arcuri et al., 2007). Research have shown that CHCP plant integration in hospital buildings is a very competitive solution in the considered tariff structure from an energetic and economic point of view in four seasons countries (Pagliarini et al., 2012). However, in spite of very encouraging scenarios, CHP practice seems not yet satisfactorily developed in the hospital field (Pagliarini et al., 2012).

This study aimed at demonstrating the use of energy integration methods, in particular by filling the gap between multi-objective process-oriented models and data assessment, in order to support engineers in the elaboration of costed energy alternatives for the development of the energy infrastructure in hospitals (DHC, heat pump, boiler, cogeneration engine, refrigeration unit, and solar thermal) over the next 7 decades.

2.3. Building Retrofit

Building retrofitting measures in hospitals have demonstrated very satisfactory results (Buonomano et al., 2014; Carbonari et al., 2015; Ascone et al., 2016), and related methods have been widely developed. Ascone et al. (2016) opted for an envelope refurbishment approach, while Buonomano et al. (2014) carried out dynamic simulations of the building envelope as well as heating, ventilation, and air conditioning (HVAC) system simultaneously, showing that the highest savings derive from retrofitting the air conditioning systems (Carbonari et al., 2015).

To investigate the benefit of retrofitting measures assessing the buildings' thermal behavior becomes crucial. In this framework, the dynamic simulation of conventional buildings has been commonly performed using software tools such as TRNSYS, EnergyPlus, IDA ICE, and others (IBPSA-USA, 2020), suitable for a small number of buildings without records of heating power profiles. More advanced building models including thermal inertia have also been largely investigated in the literature. Such methods, as the one proposed by Ashouri et al. (2015), are based on the electrical RC analogy to describe the buildings' heating demand. However, identifying the parameters of the models requires a detailed knowledge and short-time sampling of the building features such as global internal temperature, occupancy, and electricity profiles. These profiles are highly fluctuating in important public buildings, making this method

not suitable to describe districts composed of a large number of dilapidated buildings for which monitored data are not sufficient.

Therefore, due to a lack of data regarding measured and estimated energy consumption in hospital buildings (Buonomano et al., 2014), it is relevant to develop simple and yet reliable models, flexible and adaptable to large hospital complexes. This study proposes a refinement of the energy signature model (Girardin et al., 2010) to distinguish between ventilation and thermal envelope conductive heat losses, in order to take into account the hygienic prescriptions related to ventilation air flows.

2.4. Investment Scheduling in Energy Planning

Multi-time optimization problems including investment scheduling have been formulated mainly in the purpose of helping expansion planning of factories assuming fluctuating market. Garcia-Herreros et al. (2016) maximized the net present value (NPV) assuming varying prices, while Khalili-Damghani et al. (2012) proposed a multi-objective mathematical programming to select a portfolio of independent investments in the form of projects in a multi-planning period, with project parameters evolving through the time horizons. Recently, (Bütün et al. (2019), Bütün (2020) proposed an optimization approach using process integration and multiple investment periods for long-term industrial investment planning.

This work extends the methodologies above for the planning of a complex urban energy system where capital expense and timing of implementation are the key components for the selection and deployment of technologies (Bornand, 2017). The proposed multi-period description characterizes the main stages of the future district evolution by integrating refurbishment actions as decision variables of the optimization problem, thus allowing to plan improvement of the building envelope and hydronic system (**Section 3.2.1**).

3. MATERIALS AND METHODS

The proposed approach extends the use of process integration techniques to the generation of long-term energy strategy and investment planning for heterogeneous and evolving major energy consumers. Building thermal modeling techniques and state-of-the-art optimization approaches is combined and applied to a complex hospital district, the processes of which are subject to high hygienic and supply reliability constraints.

The overall demand of the hospital complex is defined by the combination of characteristic processes (**Section 3.1**), based on the results of a first stage of data monitoring and analysis, and space heating/cooling estimated through the building thermal model (**Section 3.2**). In order to apply energy integration techniques (**Section 3.4**) on evolving systems, the power heat load ($\dot{Q}$) and temperature levels (T) of all streams must be assessed in the form of composites curves ($\dot{Q}_{p,h}$, $T_{p,h}$) for typical operating periods of a year (p) over several long-term temporal horizons (h).

As space heating, cooling, and ventilation account for about one-third of the final energy consumption for hospitals located in central European climate (**Table 3**), assessing the retrofit potential of the building envelope and HVAC systems (**Section 3.3**) is a primary concern. Finally, parametric optimization is employed to generate alternative scenarios, the major underlying trends which are identified through clustering techniques (**Section 3.5**).

3.1. Hospital Processes

The main variable influencing the process power demand evolution is related to the service provided, that is, the number of patients and occupancy profile. In the case of a hospital district, processes are assumed centralized (i.e., not building-specific) and thus describe by a single degree of freedom depending on the number of patients (number of beds) or the end-use energy reference area (ERA), as process power load is daily or weekly cyclic and is approximated to be constant over the year. The temperature levels are prescribed by hygienic standards and are set as constants. The benchmark energy requirements based on a first stage of on-site data monitoring and analysis resulted in the identification of the processes presented in **Table 1**.

3.2. Heterogeneous Space Heating and Cooling

To overcome the lack of dynamic measurement and estimation of ($\dot{Q}$, T) requirements in hospital buildings, a method is proposed for the calibration of an energy model (**Section 3.2.1**) using hourly energy consumption profiles recorded on-site and initial guess of

TABLE 1 | Thermal streams overview of typical hospital processes (compiled from on-site data monitoring and analysis).

Thermal process	Material stream	Specific load	Temperatures T_{in}/T_{out} (°C)
Sanitary hot water	Water	473.9 ($Wbed^{-1}$)	10/65
Cleaning tunnels (sterilization)	Water	63.7 ($Wbed^{-1}$)	10/95
Disinfection (sterilization)	Water	169.9 ($Wbed^{-1}$)	10/55
Sterilizers	Water/steam	5.8 ($Wbed^{-1}$)	10/148
Decentralized decontamination	Water/steam	326.8 ($Wbed^{-1}$)	10/100
Server cooling	Air	153.6 ($Wbed^{-1}$)	T_{ext}/22
Medical equipment cooling	Air	326.8 ($Wbed^{-1}$)	T_{ext}/22
IRM cooling	Air	76.8 ($Wbed^{-1}$)	T_{ext}/8
Negative cold storage	Air	210.0 (Wm^{-2})	T_{ext}/-20
Positive cold storage	Air	170.0 (Wm^{-2})	T_{ext}/4
Meal production unit and cleaning	Water/steam	54.2 (Wm^{-2})	10/150
Medical research processes	Water/steam	3.0 (Wm^{-2})	10/148
Pool water	Water	207.4 (Wm^{-3})	10/35

TABLE 2 | Hospital typical end-use and hygienic standards in Switzerland. If reference is not specified corresponding values refer to data collected on-site.

Type of end-use application (k)	Area ration A_k/A_E	Internal temperature		Pulsed fresh air flow (full load)	Occupancy[a]					Electricity consumption	
		Maximum	Minimum		Occupation rate	Week		Weekend		Fans	Devices + lights
		$T_{int,min}$	$T_{int,max}$	$\dot{m}_{air,fl}$	r	t_{start}	t_{stop}	t_{start}	t_{stop}	$\dot{E}_{fan}$	$\dot{E}_{dev}$
	%	°C	°C	$m^3h^{-1}m^{-2}$	–	h				$Wm^{-3}h^{-1}$	Wm^{-2}
Medical and computing equipment	1.1	26[b]	18[b]	130[b]	1	0	0	0	0	0.14[c]	0
Administrative	12.2	26[c]	22[c]	4.86	0.6	8	18	0	0	0.34[c]	17.4[c]
Intensive care	0.3	26[b]	22[b]	14.28	1	0	24	0	24	0.55	104.5
Kitchen	0.2	30[c]	20[c]	80[c]	0.6	9	14	9	14	0.91[c]	216[c]
Laboratory/pharmacy	4.5	22[b]	24[b]	30	0.6	8	18	8	18	0.55[c]	64[c]
Medical room	5.4	26[c]	22[c]	7.2[c]	0.6	10	16	0	0	0.55[c]	36[c]
High standards medical rooms (ISO 8)	0.7	26[b]	22[b]	20	0.6	7	18	0	0	0.55	36
Operating room	0.6	24[b]	18[b]	18	1	7	18	0	0	0.55	66
Patient room	4.9	26[c]	22[c]	2.4[c]	1	0	24	0	24	0.34[c]	8.5[c]
Cold storage	0.5	–	–	0	0	0	24	0	24	0[c]	0[c]
Restaurant	1.0	26[c]	22[c]	18[c]	0.6	11	14	11	14	0.34[c]	8[c]
Isolation room	0.2	26[b]	22[b]	2.4	1	0	24	0	24	0.55	8.5
Hall + corridor	17.0	–	20[b]	0[c]	0	8	18	8	18	0[c]	7[c]
Lavatories	3.5	26.5[c]	23.5[c]	0[c]	0	10	16	10	16	0[c]	11[c]
Others	18.7	26	20	0.5	0.6	9	17	0	0	0	6
Sterilization	0.3	26[b]	20[b]	7.5	0.6	0	24	0	24	0.55	214

[a]*Ventilation required.*
[b]*SICC VA 105–1 Directive.*
[c]*SIA 2024 (grouped and averaged by similar application type) SIA (2015).*

standard parameters (**Section 3.2.2**). The method discriminates the static and dynamic space heating load (**Section 3.2.3**) in order to generate energy forecast and assess the retrofit potential of both building envelope and HVAC system in the long term (**Section 3.3**).

As the hourly energy consumption may not be available for each building, the possible lack of information is offset considering similar thermo-physical property of the building envelope and HVAC systems for given construction periods (see **Figure 1**). This approach is justified by the fact that hospital development is usually implemented by stage, with similar technical and construction materials.

3.2.1. Building Energy Model

In order to characterize the retrofit potential, it is essential to use a building model allowing to distinguish between the thermal transmission and the air renewal losses, within the building heat demand ($\dot{Q}_{hs}$). The model of **Eq. 1** is based on a quasi-static formulation (SIA, 2016) considering the thermal envelope heat transmission coefficient (U), the fresh air renewal ($\dot{m}_{air}$), and the thermal gain ($\dot{Q}_g$) from the sun, equipment, and people. Hygienic standards in public buildings, especially for hospitals, directly impose the minimum ventilation fresh air supply ($\dot{m}^{std}_{air,k}$) required for maintaining strict air quality in each area with specific end-use application (k) (Buonomano et al., 2014) and the indoor temperature range (T_{int}) required to cope with patients' low metabolic rates (Franco et al., 2017).

$$\dot{Q}_{hs} = \left[U \cdot \frac{A_{th}}{A_E} + \dot{m}_{air} \cdot c_{pair} \right] \cdot A_E \cdot (T_{int} - T_{ext}) - \dot{Q}_g \qquad (1)$$

The indoor (T_{int}) and outdoor temperature (T_{ext}), the energy reference area (A_E), and either the thermal envelope area (A_{th}) or the aspect ratio (A_{th}/A_E) are input parameters of the model. Moreover, introducing the observable external threshold temperature for heating (T_{tr}), defined by $\dot{Q}_{hs}(T_{tr}) = 0$, allows to estimate the total heat gains $\dot{Q}_g$ (**Eq. 2**) as a function of the unknown static (U) and dynamic ($\dot{m}_{air}$) parameters.

$$\dot{Q}_g = \left[U \cdot \frac{A_{th}}{A_E} + \dot{m}_{air} \cdot c_{pair} \right] \cdot A_E \cdot (T_{int} - T_{tr}) \qquad (2)$$

The supply (T_{supply}) and return temperature (T_{return}) of the hydronic distribution system in buildings are given by the set of **Eq. 3** as a function of the nominal heating power ($Q_{hs,0} = Q_{hs}(T_{ext,0} = -6°C)$) and the corresponding distribution set points ($T_{supply,0}/T_{return,0}$).

$$T_{supply} = T_{int} - \frac{Q_{hs}}{\dot{m}c_p} \cdot \frac{T_{supply,0} - T_{int}}{T_{return,0} - T_{supply,0}}$$
$$T_{return} = T_{supply} - \frac{Q_{hs}}{\dot{m}c_p} \qquad (3)$$

Equation 3 can be solved assuming a constant flow ($\dot{m}c_p = Q_{hs,0}/(T_{supply,0} - T_{return,0})$). Three sets of possible distribution set points are identified: 80/65 and 65/50°C for existing buildings, deduced from inspection of the current system, and 45/30°C assumed for the recent or refurbished ones.

3.2.2. Standard Parameter

The standard fresh air flow ($\dot{m}_{air}^{std}$) of **Eq. 4** is the weighted sum between the standard end-use fresh air flow ($\dot{m}_{air,k}^{std}$) required by each end-use application (k) and the end-use area ratio (A_k/A_E). End-use flows correspond to the full load air flow ($\dot{m}_{air,k}^{fl}$) during the period of occupancy (from $t_{k,start}$ to $t_{k,stop}$), mitigated by the occupation rate (r_k) estimated by averaging the hourly occupancy profile provided by the standards SIA 2024 (SIA, 2015) and reported in **Table 2**.

$$\dot{m}_{air}^{std} = \sum_k \dot{m}_{air,k}^{std} \cdot \frac{A_k}{A_E}$$

$$\dot{m}_{air,k}^{std} = \dot{m}_{air,k}^{fl} \cdot r_k \cdot a_{k,t} \quad \text{with} \quad a_{k,t} = \begin{cases} 1 & \text{if} \quad t_{k,start} \le t \le t_{k,stop} \\ 0 & \text{otherwise} \end{cases} \tag{4}$$

The standard building heat transfer coefficient (U^{std}) is obtained as the mean value of the heat transfer coefficient defined in SIA (2016) for different envelope components (basement walls 0.28, windows 1.3, roofs, and exterior walls 0.25 W/m^{2}K), weighted by their relative share (deduced from the on-site measurements).

The first guess for the heat gain (Q_g^{ini}) is estimated as a function of standard air flows, an envelope heat transfer coefficient, assuming a constant indoor temperature (T_{int}^{std}) and a mean observed threshold temperature close to 16°C in central Europe.

3.2.3. Parameters Estimation and Model Validation

The procedure of calibration aims at discriminating the buildings' overall static heat transfer coefficient and dynamic ventilation air flow. It consists of the following steps:

(1) Initialization of the fresh air flow, building heat transfer coefficient, and heat gains with standard values for each reference building.
(2) Estimation of the parameters using tuning factors (π_k), defined by $\dot{m}_{air} = \pi_{air} \cdot \dot{m}_{air}^{std}$, $U = \pi_U \cdot U^{std}$ and $Q_g = \pi_g \cdot Q_g^{ini}$, by fitting the model to an hourly heating consumption profile ($\dot{Q}_{hs}^{mes}$) minimizing the sum of square residuals S as by **Eq. 5**:

$$\min_{\pi_U,\pi_{air},\pi_g} S = \min_{\pi_U,\pi_{air},\pi_g} \sum_{t=1}^{n} \left(\dot{Q}_{hs}(\pi_U, \pi_{air}, \pi_g) - \dot{Q}_{hs}^{mes} \right)^2 \tag{5}$$

(3) Extrapolation of the estimated parameter to the buildings of the same cluster (**Figure 1**) for which measured data are not available.

The validity of the model is assessed by Student's test (Student, 1908) to verify the level of significance of each coefficient π_k in describing the measured data set. Following the procedure presented by Freund et al. (2006), for each coefficient, once normalized ($\tilde{\pi}_k$), the null hypothesis $H_0 : \tilde{\pi}_k = 0 \, \forall k$ is tested against the existence hypothesis $H_1 : \tilde{\pi}_k \neq 0 \, \forall k$, by computing the t-statistics and comparing it to the reference t-value. Such value is chosen according to the number of degrees of freedom of the model: the presented case is characterized by $m = 3$ variables and $n = 3{,}000$ points and therefore presents a number of degrees of freedom greater of 1,000 ($n - m - 1 > 1{,}000$), for which the reference t-value is $t_{0.95} = 1.645$. The t-statistics is computed according to the following formula:

$$t = \frac{\tilde{\pi}_k}{\sqrt{c_{kk} \cdot MSE}}, \tag{6}$$

where MSE represents the mean square error: $\frac{S}{n-m-1}$ and (c_{kk}) the k^{th} diagonal element of $C = (\tilde{X}^T \tilde{X})^{-1}$, with $\tilde{X} \in \mathbb{R}^{\mathbb{m} \times \mathbb{m}}$ being the matrix containing the normalized time series of the model variables:

$$X = \left[U \cdot A_{th} \cdot (T_{int} - T_{ext}), \dot{m}_{air} \cdot c_{pair} \cdot A_E \cdot (T_{int} - T_{ext}), \dot{Q}_g \right] \tag{7}$$

3.3. Retrofit Potential

The retrofit potential is estimated from the difference between standard and estimated values of the fresh air flow and overall envelope heat transfer coefficient. The space heating load after refurbishment ($\dot{Q}_{hs}^{ren}$) is given by **Eq. 8**.

$$\dot{Q}_{hs}^{ren} = \left[U^{std} \cdot \frac{A_{th}}{A_E} + \dot{m}_{air}^{std} \cdot c_{pair} \right] \cdot A_E \cdot (T_{int} - T_{ext}) - \dot{Q}_g \tag{8}$$

After refurbishment, the heating distribution temperatures are lowered as well with nominal departure/return temperatures of typically 55/45°C.

3.4. Energy Integration

The energy integration problem minimizes the total expense, providing the optimal match between evolving energy demand in buildings and energy conversion technologies over the long term (**Section 3.4.1**). The energy balances are expressed as linear constraint of the MILP problem (**Section 3.4.5**). Continuous variables are used for sizing technologies, while binary variables provide optimal operation and selection strategies (**Section 3.4.2**).

Long-term investment scheduling uses binary variables to define a strategy for the purchase, acquisition, upgrade, or selling of existing facilities (**Section 3.4.4**). The district development planning (**Figure 2**) is integrated as availability constraints for buildings, energy conversion technologies, and resources.

3.4.1. Cost Function

The optimal investment and operation strategy is solved through the minimization of the total cost (**Eq. 9**) over all time periods of the year (p) and long-term horizon (h).

$$\min_{y,f} TOTEX = \sum_h \left[CAPEX_h + \sum_p OPEX_{p,h} \right] \tag{9}$$

The overall operating cost ($OPEX$) over the duration of periods of year (d_p) and long-term temporal horizons (d_h) is presented in **Eq. 10**. The formulation includes the energy required by end-use applications ($\dot{E}_{p,h}^{b}$), medical equipment ($\dot{E}_{p,h}^{j}$), and the energy supplied/demanded ($\dot{Q}/\dot{E}_{p,h}^{u}$) together with maintenance cost (MC_h^u) of conversion technology units (u) of size (f_h^u), listed in **Supplementary Table S6**.

$$OPEX_{p,h} = \left[c_h^{gas} \cdot \left(\sum_{GB} \frac{\dot{Q}_{p,h}^{GB}}{\eta^{GB}} + \sum_{CHP} \frac{\dot{E}_{p,h}^{CHP}}{\eta_{el}^{CHP}} \right) + c_h^{el,buy} \cdot \left(\sum_{HP} \frac{\dot{E}_{p,h}^{HP}}{COP_{p,h}^{HP}} + \sum_{AC} \dot{Q}_{p,h}^{AC} \eta^{AC} + \sum_{b} \dot{E}_{p,h}^{b} + \sum_{j} \dot{E}_{p,h}^{j} \right) + c_h^{el,sell} \cdot \left(\sum_{CHP} \dot{E}_{p,h}^{CHP} + \sum_{PV} \dot{E}_{p,h}^{PV} \right) + c_h^{DHC} \cdot \dot{Q}_{p,h}^{DHC} + \sum_{u} MC_h^u \cdot f_h^u \right] \cdot d_p \cdot d_h, \quad (10)$$

where $\dot{E}_{p,h}^{b} = \sum_k (\dot{E}_{dev}^{k} + \dot{E}_{fan}^{k} \dot{m}_{air,k}) \cdot A_k$ represents the electricity demand associated with the end-use applications of the building (b) listed in **Table 2**, while $\sum_j \dot{E}_{p,h}^{j}$ is the aggregated electricity demand of all processes such as heavy medical devices, servers, and central processes and estimated to be 0.65kW/bed, based on observations, data monitoring, and analysis (e.g., electricity bills).

On the other hand, the overall capital expenses in each time horizon ($CAPEX_h$) is based on the formulation presented in **Eq. 11**, which assumes linear impairment loss over the equipment lifetime (lt). The investment of the selected ($y_h^u = 1$) equipment unit (u) is therefore distributed across horizons ($h \leq H$) until dismantlement ($y_H^u = 0$), assuming the resale of the equipment at the price of the residual value. In this formulation, the fixed (c_1) and variable (c_2) cost of investment are valid for installed capacity f^u in a range $[F_{min}^u, F_{max}^u]$ around the unit reference size (f_0^u), reported in **Supplementary Table S6**. The second term in the equation refers to the potential refurbishment of the generic building b.

$$CAPEX_h = \sum_u \left(c_1^u \cdot y_h^u + c_2^u \cdot f_h^u \right) \cdot \frac{d_h}{lt^u} + \sum_b c_1^{b,ren} \cdot y_h^{b,ren} \cdot \frac{d_h}{lt^b} \quad (11)$$

3.4.2. Technology Selection and Sizing

Multi-period selection and sizing of technologies allow to determine the best set of technologies, their size, and operation strategy throughout the planning horizon. The installed capacity in each temporal horizon (f_h^u) and the working load in each time step ($f_{p,h}^u$) are represented by continuous variables, while binary variables stand for the possibility to invest in technologies (y_h^u) or to refurbish buildings ($y_h^{b,ren}$) in a particular time horizon, as well as whether or not to operate technologies at certain points in time ($y_{p,h}^u$).

The system of **Eqs 12a–12c** ensures that the working load remains between specified bounds and that operation logically precedes investment in installed ($y_h^u = 1$) and used ($y_{p,h}^u \geq 1$) units.

$$y_h^u \cdot F_{min,p,h}^u \leq f_{p,h}^u \leq y_{p,h}^u \cdot F_{max,p,h}^u \quad (12a)$$

$$f_{p,h}^u \leq f_h^u \leq y_h^u \cdot F_{max}^u \qquad \forall\, u, p, h \quad (12b)$$

$$y_{p,h}^u \leq y_h^u \quad (12c)$$

3.4.3. Retrofit Actions Selection

The building heating model is implemented as a two-state entity: the current heating need ($\dot{Q}_{hs}$) (**Section 3.2.1**) and the targeted one ($\dot{Q}_{hs}^{ren}$) (**Section 3.3**) computed using standard values and achievable through retrofit actions. Additional constraints limit the use of only one building state per time horizon and period, as well as no possibility to cancel a refurbishment action. The building envelope and hydronic system are therefore either in their original state ($y_h^b = 1$) or renovated ($y_h^{b,ren} = 1$) over the whole temporal horizon (**Eqs 13a** and **13b**).

$$y_h^b + y_h^{b,ren} = 1 \quad \forall\, b, h \quad (13a)$$

$$y_{p,h}^b = y_h^b \text{ and } y_{p,h}^{b,ren} = y_h^{b,ren} \quad \forall\, b, p, h \quad (13b)$$

A renovation action, including the retrofit of the ventilation system ($y^{b,vent}$), can be activated only once and lasts for all the consecutive periods (**Eqs 14a** and **14b**).

$$y_h^{b,ren} \leq y_{h+1}^{b,ren} \quad \forall\, b, h \leq (n_h - 1) \quad (14a)$$

$$y_h^{b,vent} \leq y_{h+1}^{b,vent} \quad \forall\, b, h \leq (n_h - 1) \quad (14b)$$

The renovation of the ventilation system of a building implies the potential recovery of the heat load of the exhausted air, ideally cooled down from T_{int}^b to the ambient temperature $T_{ext} + \Delta T_{min}$. Assuming fixed LMTD equal to ΔT_{min} and constant air–air heat transfer coefficient, expenses related to the heat exchangers become proportional to the overall maximum recovered heat load, corresponding to minimum external temperature of $T_{ext,min}$= 1.6°C. Related CAPEX is thus computed according to **Eq. 11** with the unit size being the overall recovered heat load $f_h^u = \sum_b (\dot{m}_{air,b} \cdot c_{pair} \cdot (T_{int}^b - T_{ext,min} - \Delta T_{min}) \cdot y_h^{b,vent})$.

3.4.4. Long-Term Investment Scheduling

Investment scheduling aims at gradually replacing the existing facilities. The primary target influencing utility selection and sizing in public buildings, especially hospitals, is reliability in energy supply and power load backup, as presented in the list of criteria defined by Franco et al. (2017). To ensure security of supply and redundancy, a risk analysis of failure scenario defined by energy supply blackout during extreme days (winter and summer) has been simulated resulting in the definition of availability constraint (**Eqs 15a** and **15b**) ensuring a minimum capacity for backup units ($\tilde{u}$) permanently installed on-site.

$$f_h^{\tilde{u}} = f_1^{\tilde{u}} \quad \forall \tilde{u}, h \quad (15a)$$

$$y_h^{\tilde{u}} = y_1^{\tilde{u}} \quad \forall \tilde{u}, h \quad (15b)$$

Moreover, the evolution of the property master plan defines the set of temporal horizons (Figure 2). The changes are put in force by (**Eqs 16a** and **16b**) with binary parameters for construction ($a_h^b = 1$), demolition, or replacement ($a_h^b = 0$) of buildings and availability ($a_h^u = 1$) or dismantling ($a_h^u = 0$) of equipment after the lifetime limit.

$$y_{p,h}^{b|u} \leq a_h^{b|u} \quad \forall\, (b \text{ or } u), p, h \quad (16a)$$

$$y_{p,h}^{b|u} \leq a_h^{b|u} \quad \forall\, (b \text{ or } u), p, h \quad (16b)$$

Additional continuity constraints could possibly be activated for some particular units (e.g., PV and DHC) to avoid selling and to ensure constant or increasing installed capacity in time until decommissioning (**Eqs 17a–17c**)

$$y_h^u \le y_{h+1}^u \tag{17a}$$
$$f_h^u \le f_{h+1}^u \qquad \forall\, u, h \le n_h - 1 \tag{17b}$$
$$f_h^u - f_{h+1}^u \le \left(y_h^u - y_{h+1}^u\right) \cdot f_{max}^u \tag{17c}$$

3.4.5. Energy Balance

The energy integration solves the heat cascade (Gundersen, 2002), derived from all thermal streams $(\dot{Q}, T)_{p,h}$ of the problem, over the $n_{p,h}$ operating periods and n_h time horizons, as well as the overall electricity balance of **Eq. 18**.

$$\left[\sum_{HP}\frac{\dot{Q}^{HP}}{COP^{HP}} + \sum_{AC}\dot{Q}^{AC}\eta^{AC} + \sum_{b}\dot{E}^{b} + \sum_{j}\dot{E}^{j} - \sum_{CHP}\dot{E}^{CHP} - \dot{E}^{PV} - \dot{E}^{grid}\right]_{p,h} = 0 \;\forall p, h \tag{18}$$

3.5. Parametric Optimization for Scenario Generation

When optimizing for conflicting objectives, the overall optimum is not the goal (Schüler et al., 2018), and the single optimization presented in **Eq. 9** does not provide a systematic overview of the solution space. In order to generate a range of n alternative solutions, parametric optimization is used to minimize the problem with the supplementary ϵ-constraint of **Eq. 19**. The latter allows to generate different solutions for distinct values of the key performance indicator (KPI). In this study, CO_2 emissions have been chosen as the constraining KPI parameter.

$$\min_{y,f} TOTEX \text{ under constraint } KPI \le \epsilon_i$$
$$\text{with } \epsilon_i = KPI_{min} + i \cdot \frac{KPI_{max} - KPI_{min}}{n-1}, \qquad i = 0, \ldots, n-1 \tag{19}$$

3.6. Multi-Criteria Decision Analysis

The set of final system configurations (i.e., results from the last period 2030–35), obtained through the parametric optimization, is clustered using k-medoids algorithms and elbow's method. It allows for identifying the existing solution representative of the cluster. This algorithm is used instead of k-mean for preserving time continuity of the generated solutions. The scenarios identified by the cluster medoids define the main investment strategy trends and are represented by a parallel coordinate plot.

The last period is considered for defining the KPI of each solution to assess the relevance and effectiveness of the energy performance actions. The considered KPIs are the following: final energy consumption, renewable energy share, CO2 emissions, and annualized operating and investment costs.

4. CASE STUDY: UNIVERSITY HOSPITAL OF GENEVA HOSPITAL DISTRICT

4.1. Building Stock

With an annual heat and electricity consumption of 60 and 45 GWh, respectively, the HUG main complex fits the definition of "major consumer" (Republic and Canton of Geneva, 2010; Republic and Canton of Geneva, 2012). The building stock is composed of 33 buildings (25 existing and eight architectural projects within the year 2035) with an overall ERA of 332,311 m^2, and a total of 1,224 beds, including a large landscape of activities presented in **Table 2**.

Architectural projects are planned by region, dividing the district into two distinct zones: the north and south zones (see **Figure 2**). Buildings are aggregated by construction periods as shown in **Figure 1**. The distribution of the energy reference area by end-use type of activity is detailed in **Supplementary Tables S1 and S3**, and the list of project values, obtained according to **Sections 3.2** and **3.3**, is presented in **Supplementary Tables S2 and S4**.

4.2. Cost and Emissions

Considering the significant uncertainties on the cost parameters [up to 50% according to Moret et al. (2016) and Favrat et al. (2016)], a conservative approach is adopted as a first worst case estimation, setting constant energy prices to 2015 values and technology purchase costs not evolving over the studied period (2016–2035). The CO_2 emission level related to electricity consumption from the Swiss grid is set as a linearly decreasing value between 2015 and 2035, fitting the expectations of the Swiss government low-emission scenario (0.129 in 2015 down to 0.034 kg-CO_2 eq./kWh in 2035) (Favrat et al., 2016). The energy costs, emissions, and techno-economic values applied are detailed in **Supplementary Tables S5 and S6**.

The meteorological factors influencing the demand are the external temperature T_{ext} and the solar irradiation I recorded during 2015, which is taken as the reference year. Year-to-year fluctuations are neglected: a reasonable assumption considering the level of uncertainty on these parameters with respect to their sensitivity.

4.3. Property Master Plan

The property and urban project master plan define time constraints related to technology availability and renovation potential within the year 2035, as presented on the Gantt diagram (**Figure 2**). The considered 20-year long-term projection is thus divided into four time horizons of 5 years. The property master plan foresees the full renovation of the district south zone while considering partial service restructuring in the north zone. These projects can be seen as an opportunity for envelope refurbishing, and the relevance of such actions is assessed and optimized for the north zone group of buildings (orange marked entities, including 5 and 6A). Urban energy supply projects such as 4th-generation very low temperature DHC (GeniLac hydrothermal network) which are emerging in the hospital area are also included to assess the profitability of integrating them in the project.

5. RESULTS

5.1. Energy Assessment from On-Site Data Monitoring and Analysis

Energy invoices are the starting point to set the annual overall energy balance based on final energy consumption (**Table 3**; **Supplementary Figure S1**). Due to lack of monitoring of the

sanitary hot water distribution system, decentralized decontaminators, and process and equipment cooling, the corresponding consumption values are estimated from technical documentations and standards, adjusted to match annual records. Despite the fact that hospitals are large electricity consumers for lights, fans, and biomedical equipment, monitoring is not systematically performed neither on large medical equipment nor on building power consumption. Electrical power flows are therefore estimated and adjusted from invoicing, technical documentation, and the standard values defined by SIA (2015).

The composite curves of the entire hospital district (**Figure 3**) show the minimum energy requirements (MERs) in the current hospital configuration for two typical operating conditions (winter and summer), based on hospital standards [upper and lower internal temperature limitations for hospitals according to the SWKI (2015)]. It appears that MERs in winter can mainly be achieved through ventilation heat recovery systems. Half of the annual hot thermal needs are dedicated to space heating (**Table 3**), requiring a design supply temperature between 50 and 80°C due to building obsolescence. The current heat generation is centralized, and gas boilers supply heat to the entire district through a 170°C district heating network even though the sterilization process high-temperature heating needs account for only 3.8% of the overall heat consumption, as highlighted by the composite curves (**Figure 3**).

5.2. Building Thermal Model Calibration

The heating hourly power profile (**Figure 4**) and the building model calibration factors (**Table 4**) show the model relevance for describing heating needs in a typical hospital patient hosting building built in 1966. A 20% error is to be expected while computing the integral of the modeled heating power load over the full year (yearly energy bill) as summer and mid-season needs are not described by the model with the same level of accuracy.

The model calibration is performed on the reference buildings (listed in **Figure 1**) and the parameters extrapolated to the others belonging to the same cluster. Overall, 3,000 points between December 2014 and February 2015 constitute the training set.

According to **Table 4**, the null hypothesis of the three coefficients is rejected (t-value > $t_{0.95}$ = 1.645), and the model with three variables presented in **section 3.2.1** is therefore used for assessing the heating parameters of the other reference buildings. The results of the model calibration are reported in **Supplementary Table S7**.

TABLE 3 | Yearly final energy balance of the hospital district (source: on site collected data and HUG, 2016).

Supply sources		Services	
Gas and fuel oil	51%	Space heating	24.6%
		Process	13.0%
		Unidentified (losses and other)	13.4%
Cooling network	12%	Space cooling and dehumidification	5.3%
		Cold process	6.3%
Grid	37%	Refrigeration units	3.6%
		Heavy medical equipment	4.6%
		Uncontrollable load	20.3%
		Fan	7.4%
		Sparse air conditioner and compressed air	1.5%

5.3. Scenarios toward the Best Long-Term Energy Planning

The mix of solutions generated by the parametric optimization forms a Pareto front as depicted in **Figure 5**. Values of the objective function and the KPI are expressed per year and ERA in order to compare the different time horizons. The last time horizon (2030–2035) is taken as reference in order to assess the indicator's quality (**Table 5**). The parallel plot (**Figure 6**) shows each solution features in the last time horizon. The four scenarios highlight the major trends.

Scenario 1 is characterized by the full refurbishment of the whole building stock in the north zone (65% of the total ERA refurbished, **Figure 6**), leading to a large increase in the expenditures (34% higher than scenario 2 and the second most expensive). This scenario maximizes the use of SOFC fuel cells for cogeneration purposes, which is associated with a large natural gas consumption increase and a low renewable energy share (**Figure 6**).

Following the state prescriptions in terms of final energy consumption and renewable energy share, scenario 3 appears the best option, allowing for 36% final energy consumption reduction, while reducing the CO_2 emission level by 60% and decreasing the annual total cost by 24%, considering full integration of all the thermal streams (**Figure 9**). As highlighted by the parallel plot (**Figure 6**), very low–emission level solutions (scenario 1) promote the sale of all conventional gas utilities (e.g., boiler and diesel engine) in 2020, assuming full refurbishment of the north zone (**Figure 7**). These units are replaced by low-temperature utilities such as heat pumps, as well as solar thermal collectors and CHP SOFC units, to fulfill high-temperature needs (**Figures 8** and **10**). The other scenarios promote the use of reciprocating cogeneration engines combined with the SOFC fuel cell (scenario 2) or gas boiler (scenario three and 4) to supply high-temperature demand (**Figure 8**). DHC (GeniLac) is considered profitable for both heat pumping and direct cooling purposes in each scenario, the cost of this technology being assumed to be 10 cts/kWh. Each scenario favors as well the installation of multi-stage heat pumps to satisfy heating needs below 75°C, using the abovementioned DHC, together with the refurbishment of minimum 30% of the total ERA (**Figure 7**). As reference design value, about 2,000 kW water supplied at 5°C is required to feed centralized heat pumps of 4,000 kW capacity, when external temperature is of 1.7°C.

As shown by the integrated composite curves (**Figure 10**), all comfort cooling needs (4,000 kW at 12°C when the external temperature is 35°C) are fulfilled by free cooling, thanks to GeniLac DHC. This network is moreover used as a refrigeration unit hot source, for the purpose of satisfying lower temperature process needs.

The optimized investment planning (**Figure 7**) shows a transition period between 2016 and 2021, before the integration of GeniLac DHC. Equipment sizes are furthermore subject to evolve significantly up to 2026 (**Figure 8**) due to

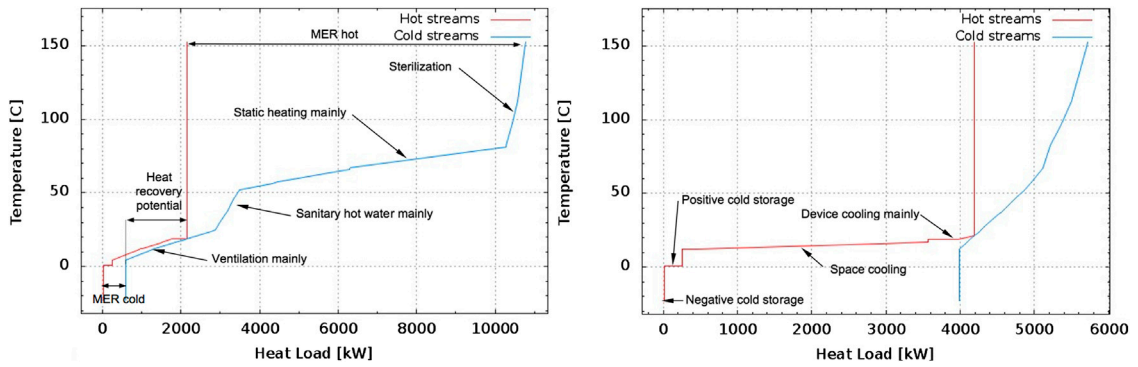

FIGURE 3 | Composite curves of the thermal streams of the entire site (energy requirements only) for two typical operating conditions: on the left, a wintertime with average external temperature of 1.7°C (February 2015) and on the right, a summertime with 24.2°C (July 2015).

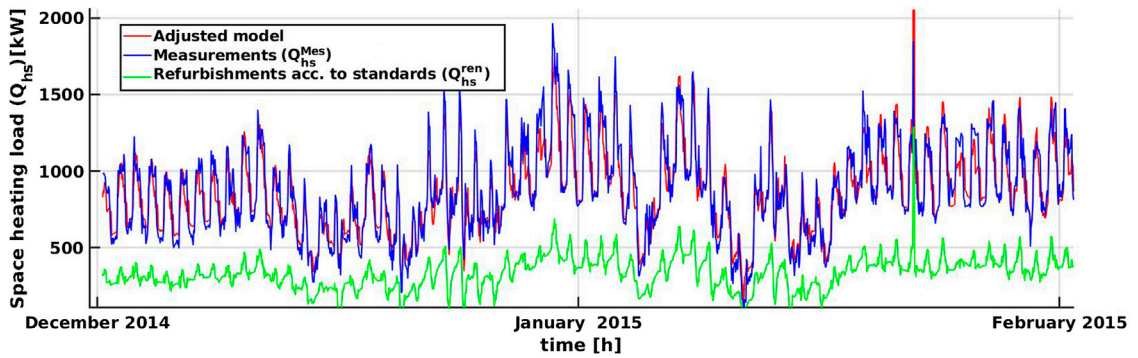

FIGURE 4 | Hourly heating consumption records (static and ventilation) in blue, calibrated model results in red, and estimated demand after refurbishment in green for the 6A patient hosting building (1966).

TABLE 4 | Parameters identification for reference building 6A with 3,000 points (December 2014 to February 2015).

Heating model parameter	Standard value[a]	Identified value[a]	π_k (—) (retrofit potential)	t-value	H_o rejected
U ($Wm^{-2}K^{-1}$)	0.6 (U^{std})	1.85	3.19	44.6	Yes
$\dot{m}_{air}$ ($m_3h^{-1}m^{-2}$)	1.3 ($\dot{m}_{air}^{std}$)	1.78	1.36	21.9	Yes
$\dot{Q}_g$ (Wm^{-2})	6.7 ($\dot{Q}_g^{ini}$)	4.29	0.64	4.1	Yes
		R^2 = 0.83			

[a]*Time-dependent values averaged over 24 h.*

TABLE 5 | ERA relative indicators increase between 2015 and 2035.

	2015 values	Scenario 1 (%)	Scenario 2 (%)	Scenario 3 (%)	Scenario 4 (%)
Yearly final energy consumption	302 ($kWh/m^2/yr$)	−32	−38	−36	−32
Yearly CO_2 emissions	52 ($kg\text{-}CO_2\text{-}eq/m^2/yr$)	−76	−73	−60	−42
Annual total cost	34 ($CHF/m^2/yr$)	+3	−20	−24	−27
Renewable energy share	20 (%)	−20	+155	+255	+150

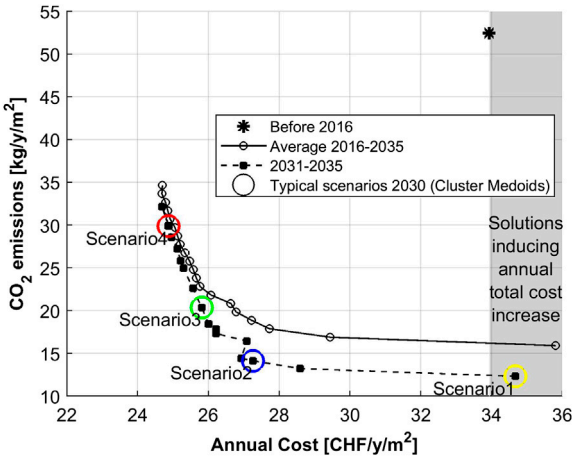

FIGURE 5 | Pareto front resulting from total costs minimization under constrained CO2 emission level. The 4 cluster medoids are extracted horizon (2031–2035). The medoids are set as reference solution for generating energy planning scenarios. The average corresponds to the sum over the four horizons between 2016 and 2035 divided by 20 years. Colors refer to **Figure 6**.

architectural morphing projects. Regarding the heat pumps, scenarios 1 to 4 promote the investment in low-temperature heat pumps (5,000 kW capacity in total supplying heat at 35°C), combined with medium-temperature heat pumps (totaling 2,000–3,000 kW capacity at 55–75°C).

5.4. Building Refurbishment Scheduling

The set of solutions emphasizes that once considered optimal for a building, refurbishment is to be conducted as the priority action (e.g., to be realized as soon as possible). Half of the heating demand being dedicated to space heating, the building obsolescence is a significant factor influencing not only the power but also the temperature levels of the heat supply systems, hence directly impacting the choice of utilities (**Figure 7**). It highlights that relevance of the refurbishment action mainly depends on three building parameters. Priority is to be given to buildings with a large aspect ratio, high heat transfer coefficient (U), and large roof area, considering that roof refurbishment expenditures are lower than facade. Since the refurbishment of the entire district is not foreseen within the considered time horizon (2017–2035), complementary units have to be considered for supplying heat at higher temperature (**Figure 10**). The results show that the entire roof surface available should be dedicated to solar thermal collectors which could bring up to 23% saving for the preparation of the sanitary hot water. Considering the moderate level of solar radiation in Geneva area, high-temperature collectors have been considered unable to supply heat at temperatures above 80°C. It is moreover estimated that distribution network renovation would allow for reaching the state prescriptions, with 30% of the sanitary water preheated by the solar collectors.

6. DISCUSSION

6.1. Toward the Minimum Energy Requirements

The minimum thermal energy requirement (237 kWh/m^2 in the current hospital configuration) is reachable by full integration of all the thermal streams, allowing a theoretical 20% savings in the yearly final energy. Implementing heat recovery on the ventilation extracted air flow (around 2,000 kW heat recovery systems to be implemented as shown in **Figure 8**) and device cooling systems appears as the most effective action to approach this target value, as demonstrated by the composite curves (**Figure 3**). Condensation heat recovery of both boiler exhaust gases and refrigeration unit hot source is to be considered too, pushing toward the implementation of a DHC in combination with heat pumping. The size of the supply pipe has to be designed according to summer free cooling needs (between 6,000 and 8,000 kW depending on the scenario).

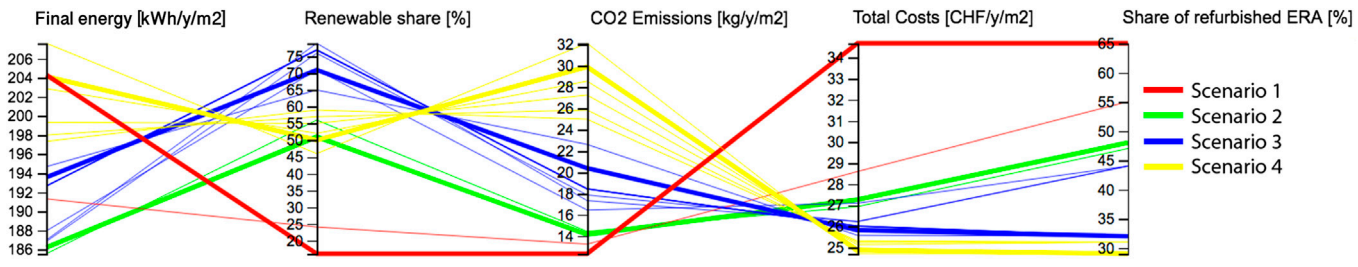

FIGURE 6 | Mix of solutions (20 lines aggregated according to the colors of **Figure 5**), the four scenarios extracted thanks to k-medoids algorithm (bold lines) and the corresponding KPI for time horizon 2030–2035.

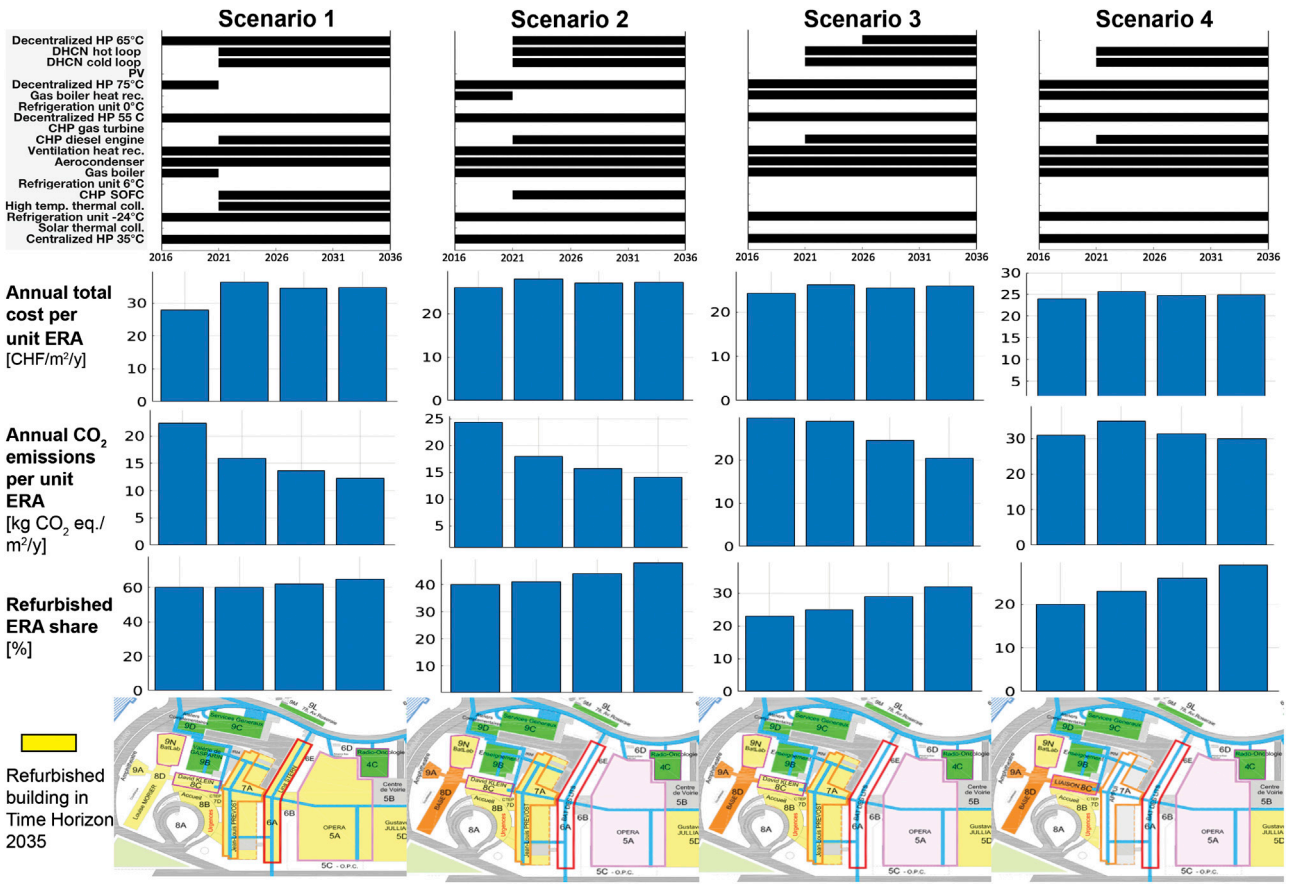

FIGURE 7 | Optimized planning related to the investment in new energy supply units and building refurbishment actions, with associated total costs at each of the four time horizon. Comparison with CO2 emissions level for each scenario. The Map of refurbishment actions aggregates all time horizons.

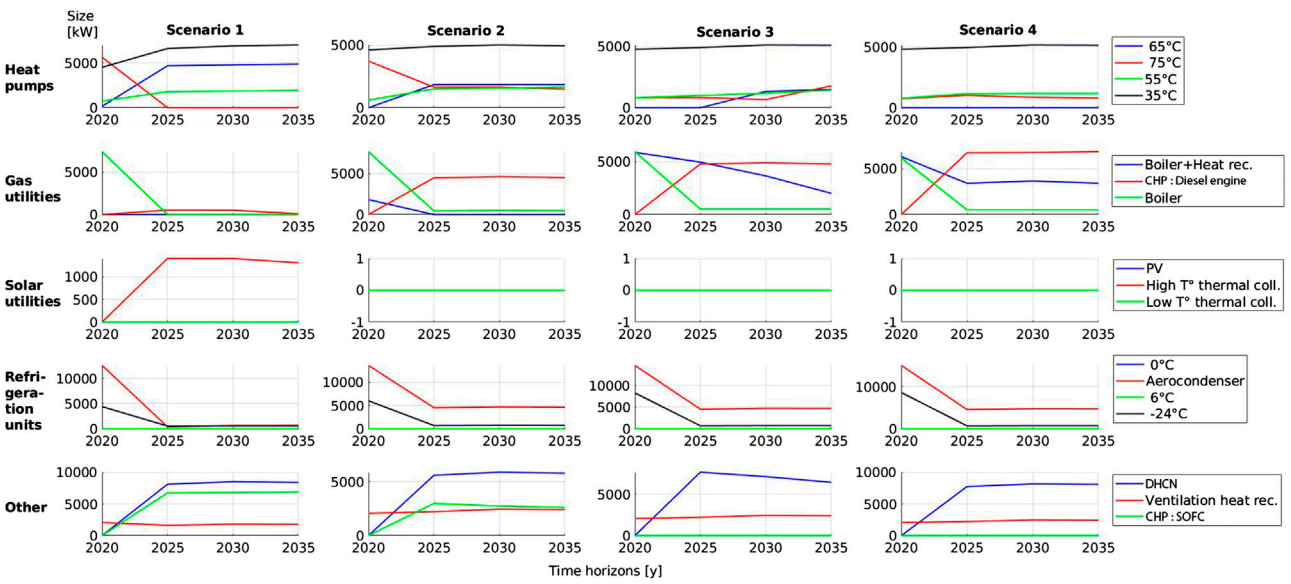

FIGURE 8 | Time evolving equipment design size over the various time horizons for each scenario.

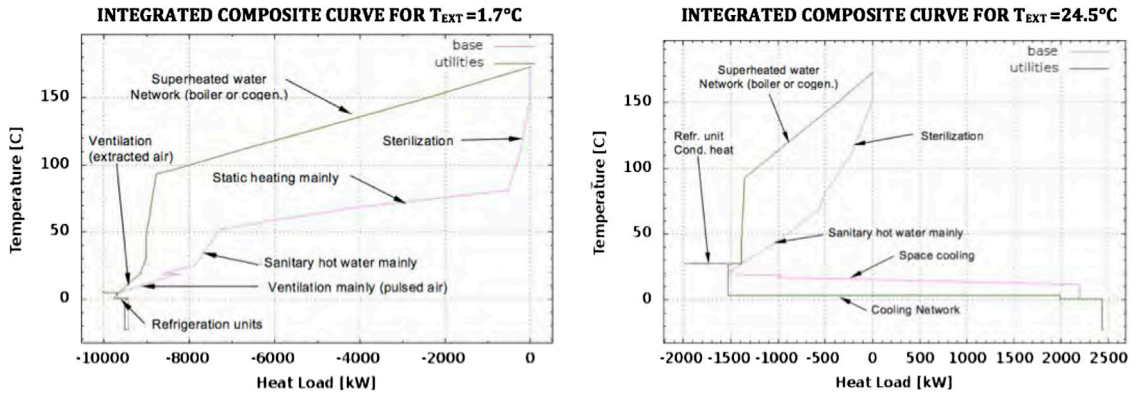

FIGURE 9 | TS Integrated Composite Curves (ICC) in current configuration (2015) for two typical wintertime and summertime operating conditions with average external temperature of February (1.7 °C) and July 2015 (24.5 °C).

The significant share of electricity consumption with respect to the overall energy demand confirms that hospitals are large electricity consumers due to heavy medical equipment, lights, fans, and numerous sparse electrical devices. And 36% of the incoming energy is thus dedicated to device operation [34% according to Franco et al. (2017)], management of which is mainly linked to user-oriented actions such as standby reduction, equipment replacement, and pooling. Therefore, the reduction of the overall energy consumption should go beyond the sole thermal aspects.

6.2. Heating Model Limitations

The building thermal model presented in **Eq. 1**, calibrated on the measured heat consumption Q_{hs}^{mes}, allows for investigating the potential of heat recovery from the exhausted air in ventilation systems of old hospital buildings, as the pulsed fresh air flow is frequently oversized (**Table 4**). The heating model being not suitable for estimating summer cooling and mid-season needs (yearly heating bill accuracy lower than 80% in these cases), its strength resides in its flexibility and the capability of being applied to complex existing buildings, for which heating parameters such as the envelope heat transmission coefficient U and average indoor temperature T_{int} are unknown and highly complex to measure.

In the framework of the current study, aiming at a preliminary analysis of the long-term investment strategy and based on monthly averaged consumption profiles, the developed model was judged accurate enough by the authors. The procedure of model calibration has however proven the interest in tuning the model parameters, rather than assuming standard values. The development of a more sophisticated thermal model, for example, being able to predict the room internal temperature and opening the doors to future analyses, such as the implementation of model predictive control systems, is left for future studies.

6.3. Investment Scheduling

Thermo-economic optimization results being highly sensitive to the chosen costing functions, an accurate characterization of the equipment and refurbishment expenditures becomes crucial. The linear formulation of the investment cost gives a satisfactory mix of solutions in terms of diversity of both technologies and investment scheduling. On the contrary, considering nonlinear

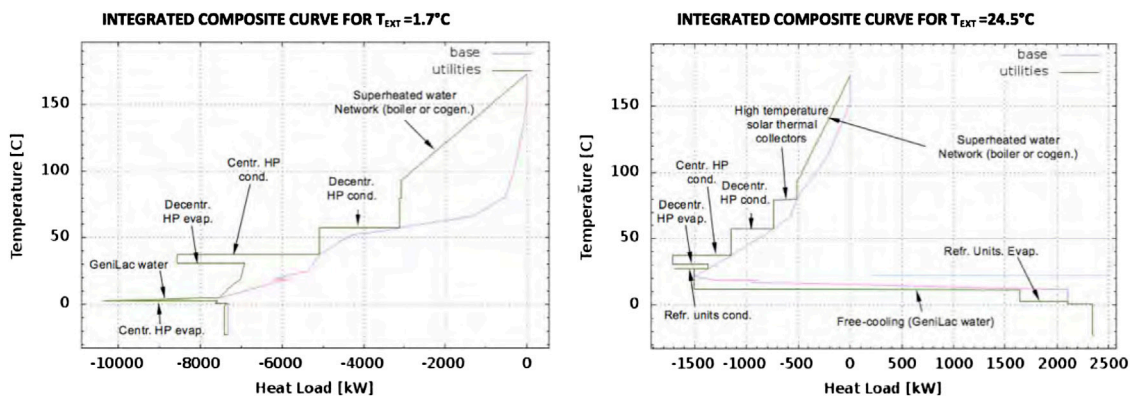

FIGURE 10 | TS integrated composite curves (ICC) of scenario 3 for time horizon 2030–2035, for two typical wintertime and summertime operating conditions with average external temperature of February (1.7°C) and July 2015 (24.5°C), considering maximum refurbishment, multi-stage heat pumps, solar thermal collectors, and GeniLac DHC.

impairment loss over the equipment lifetime would better describe the economical aspect, while adding on the other hand uncertainties related to the new parameters. Comparative studies should be carried out in order to assess the most robust formulation against uncertainties. In addition, as cost parameters have been proven to be highly subject to uncertainties [up to 50% according to Moret et al. (2016) and Favrat et al. (2016)], sensitivity analysis or robust optimization is advised, regardless of the type of costing functions employed.

Moreover, during the current study, time continuity constraints (**Eqs 17a–17c**) are neglected. Each unit is indeed considered independent from one time horizon to another, with intrinsic selling of units which once installed during the generic period h is not purchased for all the consecutive periods until the end of their lifetime. The strength of this simplistic formulation lies in the possibility of selling outdated utilities at each time horizon, promoting the energy transition toward 100% renewable utilities, as soon as the resource or technology pops up. The implementation of a more detailed selling strategy is left for future work.

6.4. Toward the Solution Design

The gains of scenario 1 regarding energy consumption and CO_2 emissions level are mitigated by the cost increase (**Table 5**). Nevertheless, other legal factors should to be considered, such as hygienic and safety standards, that will promote the hospital district full refurbishment within middle-term horizon. The state objectives regarding final energy consumption reduction and increase in renewable energy share promote the choice of scenario 3, despite a slightly higher CO_2 emission level, counterbalanced by the yearly total savings (24% of the current annual energy invoice). The corresponding energy layout for the horizon 2030–2035 is presented in **Supplementary Figure S3**.

This work aimed at proposing a methodology for the generation of a set of optimal potential solutions through parametric optimization and consequent definition of major trends by means of clustering techniques. For the presented case study, a relatively low number of solutions (20 as depicted in **Figure 5**) have been considered sufficient to achieve a satisfactory level of diversity in terms of both technological choices and KPI indicators. For other applications, depending on the problem complexity and the landscape of potential units considered, a greater number of solutions (n) in **Eq. 19** might be necessary to well-depict the solution space.

6.5. Additional Costs

The expenses related to the new heat exchangers and pipes for heat recovery and heating system retrofit are significant in the bill. Minimizing the economic impact of the network should be achieved by solving the heat exchanger network optimization problem, setting the spatiality constraints specific to the case study. Costs related to the retrofit of the hydronic network due to lowering the heating distribution temperature (**Section 3.3**) are therefore not included at this stage.

Computing the expenses related to heat recovery systems for satisfying the minimum energy requirements is a challenge due to the nonlinearity of the costs equations. These expenses have been estimated as a first approximation to be proportional to the overall heat load recovered (**Section 3.4.3**), reflecting the complexity of the case study's scale and spatiality. The network costs being however significant, better characterization of the total area of exchange and piping is a priority for future works.

6.6. Energy Supply Backup

In the current hospital configuration, backups are guaranteed by fuel oil storage (for running gas boiler and electrical power generator) and no optimization is performed on these utilities at this stage, as the implementation of such restrictive constraints directly impacts the diversity of the mix of solutions and could be investigated in a second phase. Such choice is justified considering that energy supply blackout is unlikely and short events that will only slightly affect the annual energy bill.

6.7. Integration of the Next Generation of District Networks

The implementation of SOFC fuel cells should be considered in combination with a two-phase CO_2 network, as well as SOEC reverse fuel cells with the aim of reducing gas consumption through supply–demand shifting (Suciu et al., 2018a). Dynamic models including storage and possibly thermal inertia are to be implemented in this perspective. The CO_2 network technology is suitable for space heating and cooling, while high-temperature heat generated by the fuel cell could fulfill high-hygienic standard process needs such as sterilization. The implementation of an organic Rankine cycle using the heat generated by the SOFC as hot source would allow exergy efficiency improvement, decreasing the temperature level of the stream supplied by the fuel cell to the district network.

7. CONCLUSION

The literature review carried out in the field of long-term energy planning tools has revealed a lack of studies focusing on urban major consumers. Nevertheless, results have shown that the implementation of a multi-time formulation coupled with parametric optimization appears as a powerful means to generate integration strategies for those applications characterized by complex heterogeneous building stock and evolving demand. The authors have identified the following as the main reasons:

- The investment strategy can be staged to match the evolving demand and resource availability, taking into account the architectural morphing associated to the property and state master plan.
- As half of the thermal needs of the hospital district are dedicated to space heating, while the retrofit of the building envelope implies the highest expenditures, scheduling the investment is a central aspect. Results have shown that

refurbishment appears as an action to be executed in early stages, with priority given to buildings with a large aspect ratio (as roof refurbishment is very efficient and involves moderate costs), reducing both the heating thermal load and the supply temperature of the hydronic network. This consideration justifies the use of a model able to distinguish between thermal losses and air conditioning demand and to characterize evolving heating needs over the years.
- A simple postprocessing analysis would allow to refine the investment strategy, for example, including the installation of smaller units or transition solutions to facilitate the evolution among consecutive periods.

Moreover, the parametric optimization has been proven suitable to avoid further complexity of alternative multi-objective formulations, while successfully targeting the legal prescriptions (maximal CO_2 emission level and maximal energy consumption level). The final step would be the choice by the decision-maker among the different strategies derived from the various scenarios generated by the clustering algorithm.

In the particular case study, the best mean for targeting the MER appears to be the implementation of heat recovery in the ventilation systems. The fresh air flow being generally oversized in old hospital buildings, the proposed model is suitable for buildings with global heating consumption monitored at a sampling time shorter than 24 h. Only in this case, indeed it would be possible to distinguish whether retrofitting actions are to be implemented on the ventilation system or on the building envelope and to estimate the potential benefit. Nevertheless, global static values can be easily extrapolated to other buildings of the same type with lack of energy consumption monitoring, knowing their geometrical parameters and age.

With reference to the state prescriptions in terms of maximal final energy consumption and minimal renewable energy share, very low-temperature DHC system (scenario 3) emerges among the set of solutions generated by the optimization routine, allowing for 36% final energy consumption reduction while decreasing the annual total cost by 24%. This corresponds to the most optimistic scenario regarding the renewable energy share (current values multiplied by a factor 3.5), based on a full integration of all the thermal streams (i.e., introducing heat recovery systems) including the ventilation extracted air, with a total of 2,000 kW air heat recovery systems to be implemented, the refurbishment of about 35% of the building stock, installation of 8,000 kW multi-stage heat pumping, and implementation of direct cooling through the DHC (7,000 kW hydrothermal network).

DATA AVAILABILITY STATEMENT

The data sets required to compute the model is available in the article **Supplementary Material**.

AUTHOR CONTRIBUTIONS

BB designed and implemented the methodology and models, gathered and processed the data, produced the results, and wrote the article. LG assisted in the elaboration of the method and contributed to the paper. FB contributed to the revision and improvement of the content. JLR developed the foundation of the investment planning model. SB shared its expertise in complex urban energy system management and provided the necessary on-site data and planning information. FM gave valuable hints for the elaboration of the method and the presentation of the results.

FUNDING

This project is carried out within the frame of the Swiss Center for Competence in Energy Research on the Future Swiss Electrical Infrastructure (SCCER-FURIES) with the financial support of the Swiss Innovation Agency (Innosuisse - SCCER program). Moreover, the authors would like to thank the Operations Department of the Geneva University Hospitals (HUG) for their support and assistance in collecting and making available energy measurements and other data.

SUPPLEMENTARY MATERIAL

The Supplementary Material for this article can be found online at: https://www.frontiersin.org/articles/10.3389/fenrg.2020.537973/full#supplementary-material

REFERENCES

Arcuri, P., Florio, G., and Fragiacomo, P. (2007). A mixed integer programming model for optimal design of trigeneration in a hospital complex. *Energy* 32, 1430–1447. doi:10.1016/j.energy.2006.10.023

Ascone, F., Nicola, B., Claudio, D. S., Maria, M. G., and Peter, V. G. (2016). Multi-stage and multi-objective optimization for energy retrofitting a developed hospital reference building: a new approach to assess cost-optimality. *Appl. Energy* 174, 37–68. doi:10.1016/j.apenergy.2016.04.078

Ashouri, A., Fazlollahi, S., Benz, M. J., and Maréchal, F. (2015). "Particle swarm optimization and kalman filtering for demand prediction of commercial buildings,"in Proceedings of ECOS 2015, Pau, France, June 30–July 3, 2015 Pau, France: Laboratoire de Thermique, Energetique et Procedes (LaTEP).

ASHRAE (2003). *ASHRAE handbook: heating, ventilating, and air-conditioning applications*. Atlanta, GA: American Society of Heating, Refrigerating and Air-Conditioning Engineers.

ASTM International (2017). *ASTM E917-17-standard practice for measuring life-cycle costs of buildings and building systems*. West Conshohocken, PA: ASTM International. doi:https://doi.org/10.1520/E0917-17

Biglia, A., Caredda, F. V., Fabrizio, E., Filippi, M., and Mandas, N. (2017). Technical-economic feasibility of CHP systems in large hospitals through the energy hub method: the case of cagliari AOB. *Energy Build.* 147, 101–112. doi:10.1016/j.enbuild.2017.04.047

Bornand, B. M. (2017). Integrated energy planning assistance for major consumers—application: HUG–Cluse Roseraie Hospital district. Master's thesis. Lausanne (Switzerland): IPESE-EPFL.

Buonomano, A., Calise, F., Ferruzzi, G., and Palombo, A. (2014). Dynamic energy performance analysis: case study for energy efficiency retrofits of hospital buildings. *Energy* 78, 555–572. doi:10.1016/j.energy.2014.10.042

Bütün, H., Kantor, I., and Maréchal, F. (2019). An optimisation approach for long-term industrial investment planning. *Energies* 12, 4076. doi:10.3390/en12214076

Bütün, H. E. (2020). Optimal retrofit and investment planning methodologies for improving industrial energy and resource efficiency. Thesis. Lausanne (Switzerland): EPFL. doi:10.5075/epfl-thesis-7231

Cajot, S., Peter, M., Bahu, J.-M., Guignet, F., Koch, A., and Maréchal, F. (2017). Obstacles in energy planning at the urban scale. *Sustain Cities Soc.* 30, 223–236. doi:10.1016/j.scs.2017.02.003

Cajot, S., and Schüler, N. (2019). "Urban energy system planning: overview and main challenges," in *Urban energy systems for low-carbon cities*. Editor U. Eicker (Cambridge, MA Academic Press), 19–49. doi:10.1016/B978-0-12-811553-4.00001-9

Carbonari, A., Fioretti, R., Lemma, M., and Principi, P. (2015). Managing energy retrofit of acute hospitals and community clinics through EPC contracting: the MARTE project. *Energy Proc.* 78, 1033–1038. doi:10.1016/j.egypro.2015.11.054

Favrat, D., Codina Gironès, V., Vuille, F., and Maréchal, F. (2016). "The information platform energyscope.ch on the energy transition scenarios," in Proceedings of ECOS 2016, Portoroz, Slovenia, June 19–23, 2016, Faculty of Mechanical Engineering, Ljubljana.

Favrat, D., Marechal, F., and Epelly, O. (2008). The challenge of introducing an exergy indicator in a local law on energy. *Energy* 33, 130–136. doi:10.1016/j.energy.2007.10.012

Fazlollahi, S. (2014). Decomposition optimization strategy for the design and operation of district energy systems. Thesis. Lausanne (Switzerland): EPFL. doi:10.5075/epfl-thesis-6130

Franco, A., Shaker, M., Kalubi, D., and Hostettler, S. (2017). A review of sustainable energy access and technologies for healthcare facilities in the global south. *Sustainable Energy Technol. Assess.* 22, 92–105. doi:10.1016/j.seta.2017.02.022

Freund, R., Wilson, W., and Sa, P. (2006). *Regression analysis*. 2nd Edn. New York, NY: Elsevier.

Garcia-Herreros, P., Zhang, L., Misra, P., Arslan, E., Mehta, S., and Grossmann, I. E. (2016). Mixed-integer bilevel optimization for capacity planning with rational markets. *Comput. Chem. Eng.* 86, 33–47. doi:10.1016/j.compchemeng.2015.12.007

Girardin, L., Lepage, L., and Doppenberg, F. (2015). "A supply/demand decision making-tool for the regional coordinated planning of thermal networks," in CISBAT 2015 International Conference "Future Buildings and Districts - Sustainability from Nano to Urban Scale", Lausanne, Switzerland, September 9-11, 2015 (Lausanne, EPFL Solar Energy and Building Physics Laboratory), 785–790. doi:10.5075/epfl-cisbat2015-785-790

Girardin, L., Maréchal, F., Dubuis, M., Calame-Darbellay, N., and Favrat, D. (2010). Energis: a geographical information based system for the evaluation of integrated energy conversion systems in urban areas. *Energy* 35, 830–840. doi:10.1016/j.energy.2009.08.018

Gundersen, T. (2002). *A process integration PRIMER*. Trondheim (Norway): International Energy Agency (SINTEF Energy Research, Department of Thermal Energy and Hydro Power. Available at: https://iea-industry.org/app/uploads/a-process-integration-primer-iea-t-gundersen_2002.pdf.

Gynther, L., Lapillonne, B., and Pollier, K. (2015). Energy efficiency trends and policies in the household and tertiary sectors—an analysis Based on the ODYSSEE and MURE databases (ODYSSEE-MURE project). Available at: http://www.odyssee-mure.eu/publications/br/energy-efficiency-trends-policies-buildings.pdf.

Hakim, M., Walia, H., Dellinger, H. L., Balaban, O., Saadat, H., Kirschner, R. E., et al. (2018). The effect of operating room temperature on the performance of clinical and cognitive tasks. *Pediatr. Qual. Saf.* 3, e069. doi:10.1097/pq9.0000000000000069

Herrera, A., Islas, J., and Arriola, A. (2003). Pinch technology application in a hospital. *Appl. Therm. Eng.* 23, 127–139. doi:10.1016/S1359-4311(02)00157-6

HUG (2016). Hôpitaux Universitaires de Genève, Rapport d'activité 2015. Genève: HUG - Direction de la communication. Available at: https://www.hug.ch/sites/interhug/files/documents/hug-ra2015_0.pdf

IBPSA-USA (2020). Building energy software tools—formerly hosted by US Dept. of Energy. Available at: https://www.buildingenergysoftwaretools.com [Dataset] (Accessed January 27, 2020).

IEA (2018). 2018 Global status report: towards a zero-emission, efficient and resilient buildings and construction sector. Paris, France: International Energy Agency. Available at: http://hdl.handle.net/20.500.11822/27140

IRENA (2018). *Global energy transformation: a roadmap to 2050*. Abu Dhabi: International Renewable Energy Agency (IRENA).

Khalili-Damghani, K., Tavana, M., and Sadi-Nezhad, S. (2012). An integrated multi-objective framework for solving multi-period project selection problems. *Appl. Math. Comput.* 219, 3122–3138. doi:10.1016/j.amc.2012.09.043

Liew, P. Y., Theo, W. L., Wan Alwi, S. R., Lim, J. S., Abdul Manan, Z., Klemeš, J. J., et al. (2017). Total site heat integration planning and design for industrial, urban and renewable systems. *Renew. Sustain. Energy Rev.* 68, 964–985. doi:10.1016/j.rser.2016.05.086

Liew, P. Y., Walmsley, T. G., Wan Alwi, S. R., Abdul Manan, Z., Klemeš, J. J., and Varbanov, P. S. (2016). Integrating district cooling systems in locally integrated energy sectors through total site heat integration. *Appl. Energy* 184, 1350–1363. doi:10.1016/j.apenergy.2016.05.078

Moret, S., Bierlaire, M., and Maréchal, F. (2016). Robust optimization for strategic energy planning. *Informatica* 27, 625–648. doi:10.15388/Informatica.2016.103

Murdock, H. E., Gibb, D., André, T., Appavou, F., Brown, A., Epp, B., et al. (2019). Renewables 2019 global status report. Paris: REN21 Secretariat. . Available at: https://www.ren21.net/wp-content/uploads/2019/05/gsr_2019_full_report_en.pdf

Pagliarini, G., Corradi, C., and Rainieri, S. (2012). Hospital CHCP system optimization assisted by TRNSYS building energy simulation tool. *Appl. Therm. Eng.* 44, 150–158. doi:10.1016/j.applthermaleng.2012.04.001

Rager, J. M. F. (2015). Urban energy system design from the heat perspective using mathematical programming including thermal storage. Thesis. Lausanne, (Switzerland): EPFL. doi:10.5075/epfl-thesis-6731

Republic and Canton of Geneva (2010). Loi sur l'énergie (LEn) (State of Geneva). Available at: https://www.ge.ch/legislation/rsg/f/s/rsg_l2_30.html

Republic and Canton of Geneva (2012). Règlement d'application de la loi sur l'énergie (REn) (State of Geneva). Available at: https://www.ge.ch/legislation/rsg/f/s/rsg_L2_30P01.html

Schüler, N., Cajot, S., Peter, M., Page, J., and Maréchal, F. (2018). The optimum is not the goal: capturing the decision space for the planning of new neighborhoods. *Front. Built Environ.* 3, 76. doi:10.3389/fbuil.2017.00076

SIA (2015). *Cahier technique SIA 2024, Données d'utilisation des locaux pour l'énergie et les installations du bâtiment*. Zurich: Swiss Society of Engineers and Architects (SIA).

SIA (2016). *Sia 380/1:2016 - besoins de chaleur pour le chauffage*. Zurich: Swiss Society of Engineers and Architects (SIA).

Student (1908). The probable error of a mean. *Biometrika* 6, 1–25. doi:10.2307/2331554. Available at: http://www.jstor.org/stable/2331554

Suciu, R., Girardin, L., and Maréchal, F. (2018a). Energy integration of CO_2 networks and power to gas for emerging energy autonomous cities in Europe. *Energy* 157, 830–842. doi:10.1016/j.energy.2018.05.083

Suciu, R., Stadler, P., Girardin, L., and Maréchal, F. (2018b). "Multi-period multi-time optimisation of co_2 based district energy systems," in Proceedings of ESCAPE 28, Graz, Austria, June 10–13, 2018 (Elsevier), 1057–1062. doi:10.1016/B978-0-444-64235-6.50185-6

SWKI (2015). DIRECTIVE SICC VA105-01, Installations de ventilation et climatisation pour les locaux utilisés à des fins médicales (planification, réalisation, qualification, exploitation). Schönbühl: Schweizerischer Verein von Gebäudetechnik-Ingenieure (SWKI).

Teke, A., and Timur, O. (2014). Assessing the energy efficiency improvement potentials of HVAC systems considering economic and environmental aspects at the hospitals. *Renew. Sustain. Energy Rev.* 33, 224–235. doi:10.1016/j.rser.2014.02.002

Wang, T., Li, X., Liao, P.-C., and Fang, D. (2016). Building energy efficiency for public hospitals and healthcare facilities in China: barriers and drivers. *Energy* 103, 588–597. doi:10.1016/j.energy.2016.03.039

Weber, C. I. (2008). Multi-objective design and optimization of district energy systems including polygeneration energy conversion technologies. Thesis. Lausanne (Switzerland): EPFL. doi:10.5075/epfl-thesis-4018

Yoo, M.-J., Lessard, L., Kermani, M., and Maréchal, F. (2015). OsmoseLua-an integrated approach to energy systems integration with LCIA and GIS. *Comput. Aided Chem. Eng.* 37, 587–592. doi:10.1016/B978-0-444-63578-5.50093-1

Conflict of Interest: The authors declare that the research was conducted in the absence of any commercial or financial relationships that could be construed as a potential conflict of interest.

The reviewer AK declared a shared publication, though no other collaboration, with one of the authors FM to the handling Editor.

GLOSSARY

Acronyms

AC aerocondenser

APE energy performance action

CAPEX capital expenditure

CHP combined heat and power

CHUV University Hospital of Lausanne

CMU Center for Medical Research

COP coefficient of performance

DHC district heating and cooling

ERA energy reference area

GB gas boiler

HP heat pump

HR ventilation heat recovery system

HUG University Hospital of Geneva

HVAC heating ventilation and air conditioning

KPI key performance indicator

MC maintenance cost

MCDA multi-criteria decision analysis

MER minimum energy requirements

MILP mixed-integer linear programming

MSE mean square error

NPV net present value

OPEX operating expenditure

PV photovoltaic panels

RC electrical resistor–capacitor

SC solar (thermal) collectors

SIG Industrial Services of Geneva

SOEC sold oxide electrolysis cell

SOFC solid oxide fuel cell

TC solar thermal collectors

UCPD meal production centralized unit

Symbols

$\dot{E}$ electrical load, kW

$\dot{m}$ mass flow, kg/s

$\dot{Q}$ thermal load, kW

η equipment efficiency

π model parameter tuning factor

a binary parameter

A_E energy reference area

A_{th} building's thermal envelope area

A_{th}/A_E building's aspect ratio

c operation cost, CHF/KWh

c_1 fixed investment, CHF

c_2 variable investment, CHF/KW

c_p specific heat, J/(kg K)

d time duration, h

F capacity limit, kW

f equipment size, kW

i interest rate

lt lifetime, years

R heat cascade residuals, kW

r occupation rate, %

S sum of square residuals

T temperature, K

U conductive heat transfer coefficient, W/(m^{2}K)

y binary variable

Subscripts/Superscripts

0 design condition

b index of building

dev electrical device

el electrical

ext external (outdoor)

fan ventilation fan

fl full load

h index of time-horizon

hs heating system

ini initial guess

int internal (indoor)

j index of process

k index for end-use application

mes measured

p index of time-period

ren renovated

s stream

std standards value

tr threshold

u index of energy conversion utility

vent ventilation system